Desalination and Water Treatment
www.deswater.com
1944-3994/1944-3986 © 2012 Desalination Publications. All rights reserved
doi: 10/5004/dwt.2012.3101

Taylor & Francis
Taylor & Francis Group

44 (2012) 229–236
June

Phosphate removal from aqueous solutions using slag microspheres

Chang-Gu Lee[a], Jeong-Ann Park[a], Song-Bae Kim[b,*]

[a]*Environmental Biocolloid Engineering Laboratory, Seoul National University, Seoul 151-921, Korea*
[b]*Department of Rural Systems Engineering/Research Institute for Agriculture and Life Sciences, Seoul National University, Seoul 151-921, Korea*
Tel. +82 2 880 4587; Fax: +82 2 873 2087; email: songbkim@snu.ac.kr

Received 11 July 2011; Accepted 2 January 2012

ABSTRACT

The objective of this study was to investigate phosphate removal from aqueous solutions using slag microspheres produced from converter furnace steel slag (CFSS) via a slag atomizing process. Batch and column experiments were performed to examine phosphate removal efficiency of the slag microspheres. X-ray fluorescence analysis indicated that the slag microspheres were composed of calcium (40.7%) and iron (25.1%) as well as silica (SiO_2), magnesium, aluminum, and manganese. X-ray diffractometer patterns demonstrated that srebrodolskite (dicalcium ferrite, $Ca_2Fe_2O_5$), magnetite (Fe_3O_4), and hematite (Fe_2O_3) were the major constituents of the slag microspheres. Based on kinetic experiments, the reaction reached equilibrium after around 9 h. Based on equilibrium experiments, the maximum removal capacity was 10.95 mgP g^{-1} from the Langmuir–Freundlich isotherm model. When the solution pH was increased from 3.2 to 9.2, the removal capacity decreased by one order of magnitude from 3.16 ± 0.04 to 0.35 ± 0.15 mgP g^{-1}. This indicates that adsorption on metal hydroxide surfaces may play a major role in the phosphate removal process using slag microspheres. The decreasing tendency of removal capacity with increasing pH may be attributed to the surface charge of the slag microspheres, which have a point of zero charge (PZC) of 7.6. These results also demonstrated that nitrate (NO_3^-), chloride (Cl^-), and sulfate (SO_4^{2-}) had minimal effects on the removal of phosphate at anion concentrations ranging from 0 to 100 mM while bicarbonate greatly interfered with the removal of phosphate resulting in a 87% reduction of the removal capacity. In column experiments, a phosphate removal capacity of 2.27 mgP g^{-1} was achieved (initial phosphate concentration = 200 mgP l^{-1}). This study demonstrates the potential use of slag microspheres as granular filter media in flow-through systems for phosphate removal.

Keywords: Slag microspheres; Phosphate removal; Sorption; Batch experiment; Column experiment

1. Introduction

Low cost and widely available adsorbents for contaminant removal can be obtained from agricultural and industrial by-products. Iron/steel slags are produced in large quantities as by-products of iron/steel manufacturing processes. Iron/steel slags are classified into blast furnace iron slag (BFIS) and basic oxygen furnace steel slag (BOFSS). BFIS is produced during the iron production process, in which iron ores react with lime as a fluxing agent in a blast furnace to generate molten iron. BFIS is primarily composed of silica (SiO_2) and

*Corresponding author.

alumina (Al_2O_3) along with calcium and magnesium oxides (CaO, MgO). BOFSS is generated during the steel-making process in which molten iron is converted into steel using oxygen in a basic oxygen furnace. BOFSS has a similar chemical composition to BFIS but has higher iron and manganese oxides contents (FeO, MnO). BOFSS is further divided into converter furnace steel slag (CFSS) and electric arc furnace steel slag (EAFSS), depending on the type of furnace from which it is generated. Iron/steel slags are commonly used as road bed materials, cement additives, landfill cover materials, and contaminant adsorbents [1–3].

The pollution of water bodies by phosphorus, an essential macronutrient, is a widespread environmental problem, causing eutrophication in lakes and seas and posing a serious threat to aquatic environments. Iron/steel slags have been used by several researchers to investigate the removal of phosphate from aqueous solutions [4–12]. Some researchers have used BFIS to evaluate phosphate removal in synthetic wastewater and the secondary effluent from activated sludge processes using column experiments [13,14], the phosphate removal mechanism and hydroxyapatite [$Ca_{10}(OH)_2(PO_4)_6$] formation from calcium-phosphate precipitation [15], the effects of pH, temperature, agitation rate, and dosage of BFIS on phosphate removal [16,17], methodological aspects of BFIS application in phosphate removal strategies using batch and pilot-scale experiments in phosphate solutions and municipal wastewater [18], and the effect of hydrated lime addition on the phosphate removal efficiency [19]. Others have utilized BOFSS for the removal of phosphate from aqueous solutions to investigate the phosphate retention capacity of EAFSS using long-term column experiments in a synthetic phosphate solution [20,21], phosphate recovery from wastewater using CFSS via hydroxyapatite crystallization [22–24], phosphate removal by slag filter at a full-scale treatment plant [25], and the phosphate adsorption characteristics on BOFSS as a function of pH, ionic strength, and initial P concentration [3,26]. These studies demonstrated that iron/steel slags are valuable industrial by-products, which can be used for phosphate removal from aqueous solutions via adsorption and/or precipitation mechanisms. Phosphate can be adsorbed on metal (Al, Fe) hydroxides on the surfaces of slags. Also, phosphate can form stable phosphate precipitates such as hydroxyapatite ($Ca_{10}(PO_4)_6(OH)_2$) with calcium ions [3,8].

Slags are not stable but expand in water due to the hydration of free CaO from slags [26,27]. To produce granular filter media with mechanical strength and stability, slags can be further processed via slag atomizing technology. During processing, the amount of free CaO in the slags is reduced while slag microspheres are formed.

The objective of the present study was to investigate the removal of phosphate from aqueous solutions using slag microspheres produced from CFSS via a slag atomizing process. Batch and column experiments were performed to evaluate the removal of phosphate in the slag microspheres.

2. Materials and methods

2.1. Slag microspheres

Slag microspheres supplied by Ecomaister, Korea were passed through US standard sieve (Dong Ah Testing Machine Co., Seoul, Korea) numbers 30 and 16, and only the fraction with grain sizes of 0.60–1.18 mm was used in the subsequent experiments. The true density and bulk density of slag microspheres were determined using the Korean Standard Testing Method (KS F2504 and KS F2505, respectively), and the porosity was calculated using the true density and bulk density. A field emission scanning electron microscope (FESEM) combined with an energy dispersive X-ray spectrometer (EDS) analyses were performed to examine the surface structure of the slag microspheres by X-ray microanalysis, as described previously [28]. Briefly, specimens were mounted on metal stubs using carbon tape and were sputter-coated with platinum to a thickness of approximately 20 nm. The specimens were examined with a FESEM (Supra 55VP; Carl Zeiss, Oberkochen, Germany) at an accelerating voltage of 3 kV. In addition, the elemental composition was determined with an EDS (XFlash 4000; Bruker AXS, Berlin, Germany) combined with an electron microscope at an accelerating voltage of 15 kV. X-rays were collected using a detector fixed at a take-off angle of 35°. In addition, the powdered form of the slag microspheres was characterized using a powder X-ray diffractometer (XRD D5005, Bruker AXS, Berlin, Germany) with Cu Kα radiation (1.5406 Å) at a scanning speed of 0.6° s^{-1}. The chemical composition was investigated using an X-ray fluorescence spectrometer (XRF-1700, Shimadzu Co., Japan). The point of zero charge (PZC) was determined by measuring the zeta potential at various pH values, which were obtained using dilute HNO_3 and NaOH.

2.2. Batch experiments

Phosphate removal in the slag microspheres was evaluated by conducting kinetic and equilibrium batch experiments. The desired phosphate solution was prepared by diluting the stock solution (1000 mgP l^{-1}) made from potassium dihydrogen phosphate (KH_2PO_4) with deionized water and 20 mM KNO_3. The slag microspheres (1.0 g) were added into a 50 ml polypropylene

conical tube containing 30 ml of the phosphorus solution. The tube was shaken at 30°C and 100 rpm using a shaking incubator (Daihan Scientific, Korea). The high initial phosphorus concentration (200 mgP l^{-1}) was selected based on the preliminary tests to quantify the performance of the slag microspheres in the removal of phosphate. The kinetic experiments were performed at an initial phosphorus concentration of 200 mgP l^{-1} (Ph = 5.1). Then, samples were taken 1.5, 3, 6, 9, 12, 24, 36, 48, and 60 h after the start of the reaction. The experiments were performed in triplicate. Equilibrium tests were conducted with initial phosphorus concentrations ranging from 75 to 1000 mgP l^{-1}. The samples were collected 9 h post-reaction and filtered through a 0.45 μm membrane filter. The effects of the initial pH (3–10) and competing ions on the phosphorus removal were also investigated. NO_3^-, Cl^-, SO_4^{2-}, and bicarbonate solutions were prepared by dissolving KNO_3, KCl, K_2SO_4, and $KHCO_3$, respectively, in deionized water. These samples were also collected 9 h post-reaction and filtered through a 0.45 μm membrane filter. The phosphate was analyzed by the ascorbic acid method [29]. The phosphate concentration was measured at a wavelength of 880 nm using a UV–vis spectrophotometer (Helios, Thermo Scientific, Waltham, MA, USA). The pH was measured with a pH probe (9107BN, Thermo Scientific, Waltham, MA, USA). The amount of phosphorus adsorbed on the slag microspheres (q, mgP g^{-1}) was calculated using the following equation:

$$q = (C_i - C_f) \times \frac{V}{m} \quad (1)$$

where C_i and C_f are the initial and final concentrations of the phosphorus in solution (mgP l^{-1}), respectively, V is the solution volume (l), and m is the mass of the slag microspheres (g).

2.3. Column experiments

Column experiments were performed using a Plexiglas column (inner diameter = 5.0 cm, bed depth = 30 cm) packed with quartz sand (particle size = 0.5–2.0 mm; mass of filter media = 1020 g) and slag microspheres (mass of filter media = 1380 g). Prior to the experiments, the packed column was flushed upward using a HPLC pump (Series α pump, Scientific Systems Inc., State College, PA, USA) operating at a rate of 2.0 ml min^{-1} using five bed volumes of deionized water until steady state flow conditions were established. Then, the phosphate solution was introduced to the packed column at the same flow rate. Portions of the effluent were collected using an auto collector (Retriever 500, Teledyne, City of Industry, CA, USA) at regular intervals and the phosphate was analyzed using the ascorbic acid method [29]. The mass of phosphate removed per unit mass of the slag microspheres in the column [phosphate removal capacity of the slag microspheres, q_a (mgP g^{-1})] was determined using the following equation:

$$q_a = \frac{C_{cap}}{M_f} \quad (2)$$

where M_f is the mass of the slag microspheres and C_{cap} is the column capacity for phosphate removal at a given flow rate and influent phosphate concentration.

3. Results and discussion

3.1. Characteristics of the slag microspheres

The physical properties and chemical compositions of the slag microspheres are presented in Table 1. The slag microspheres were composed of calcium (40.7%) and iron (25.1%) as well as SiO_2, magnesium, aluminum, and manganese. The microspheres had a true density of 3.56 g cm^{-3} and a porosity of 0.363. Digital and FESEM images along with the EDS patterns are shown in Fig. 1. The slag microspheres were black and were round in shape with rough surfaces. The EDS pattern indicates that Ca was evident at peak positions of 3.69 and 4.01 keV as K alpha and K beta X-ray signals, respectively. Fe was found at peak positions of 0.70, 6.40, and 7.06 keV as L alpha, K alpha, and K beta X-ray signals, respectively. In addition, Mg and Al were found at 1.25 and 1.48 keV, respectively, as K alpha X-ray signals. The XRD pattern demonstrated that srebrodolskite (dicalcium ferrite, $Ca_2Fe_2O_5$), magnetite (Fe_3O_4), and hematite (Fe_2O_3) were the major constituents of the slag microspheres (Fig. 2).

Table 1
Physical properties and chemical compositions of the slag microspheres used in this study

Physical properties				Chemical compositions (%)					
Particle size (mm)	True density (g cm^{-3})	Bulk density (g cm^{-3})	Porosity (–)	SiO_2	Al_2O_3	CaO	MgO	Fe_2O_3/FeO	MnO
0.60–1.18	3.56	2.27	0.365	10.3	2.0	40.7	8.8	25.1	1.0

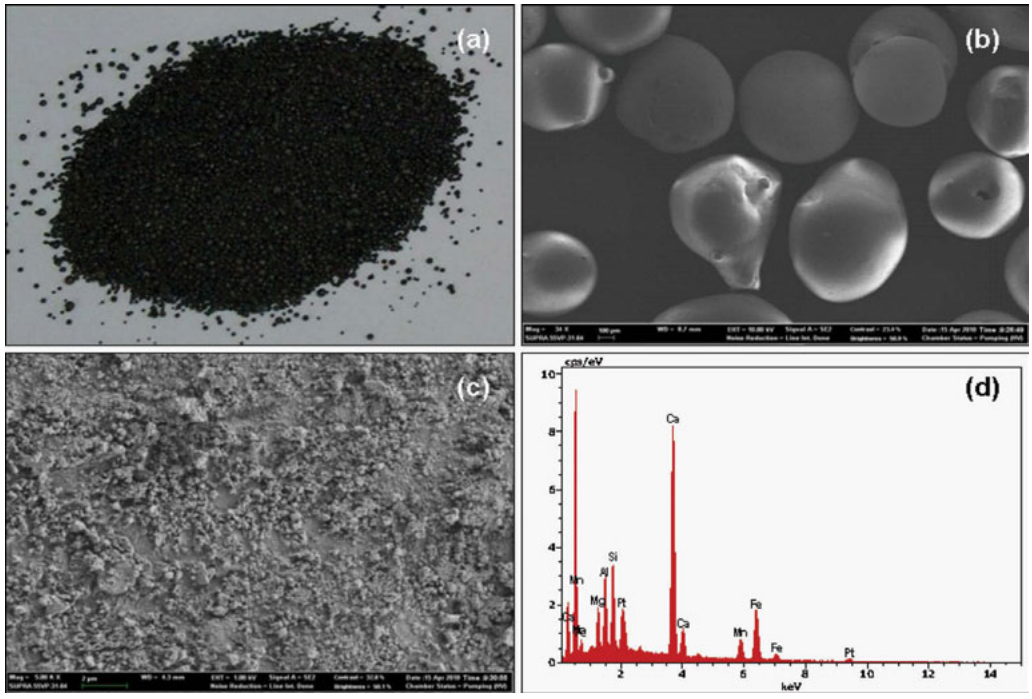

Fig. 1. (a) Digital image, (b) field emission scanning electron micrograph (FESEM) image (bar = 100 μm), (c) FESEM image (bar = 2 μm), and (d) X-ray spectrum (EDS) of the slag microspheres.

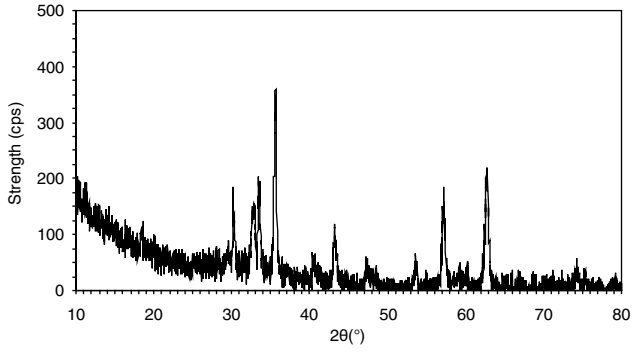

Fig. 2. X-ray diffraction pattern (XRD) of a powdered form of the steel slag microspheres.

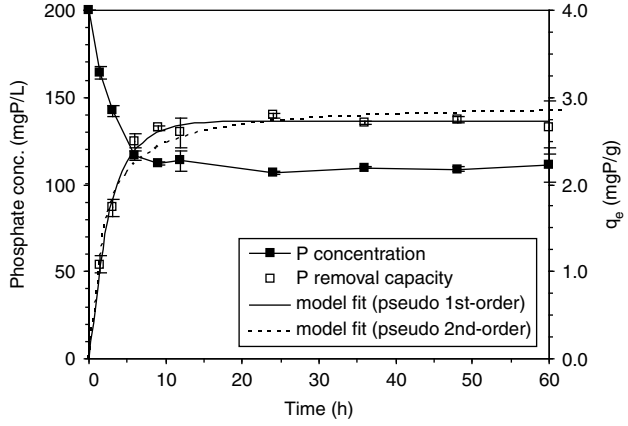

Fig. 3. Kinetic batch data and model fit for phosphate removal by the slag microspheres (initial phosphate concentration = 200 mgP l^{-1}).

3.2. Removal kinetics

The kinetic removal data of phosphate in the slag microspheres is shown in Fig. 3. In the initial phase, the phosphate concentration decreased quickly from 200 to 142 mgP l^{-1} after 3 h. The average percentage removal of phosphate after 3 h was 29%. The reaction reached equilibrium at around 9 h with a corresponding phosphate concentration of 111 mgP l^{-1}. At that time, the average removal percent was 44%. The kinetic removal data were analyzed by applying pseudo first-order and pseudo second-order models [30,31], as shown below:

$$q_t = q_e \left[1 - \exp\left(-k_1 t\right)\right] \quad (3)$$

$$\frac{1}{q_e - q_t} = \frac{1}{q_e} + k_2 t \quad (4)$$

In these equations, q_t is the amount of phosphate removed at time t, q_e is the amount of phosphate removed at equilibrium, k_1 is the pseudo first-order rate constant, and k_2 is the pseudo second-order velocity constant. The kinetic model parameters are provided in Table 2. In the pseudo first-order model, the value of k_1 was 0.35 1 h^{-1} while the value of q_e was 2.73 mgP g^{-1}. In the pseudo second-order model, the value of k_2 was

Table 2
Kinetic model parameters for the pseudo first-order and pseudo second-order models in the kinetic batch experiments (initial phosphate concentration = 200 mgP l^{-1})

Model parameter	Pseudo first-order model			Pseudo second-order model		
	k_1 (1 h^{-1})	q_e (mgP g^{-1})	R^2	k_2 (g mgP^{-1} h^{-1})	q_e (mgP g^{-1})	R^2
Value	0.35	2.73	0.99	0.18	2.93	0.92

0.18 g mgP^{-1} h^{-1}. The value of q_e was 2.93 mgP g^{-1}, which is slightly higher than that obtained from the pseudo first-order model. Based on the correlation coefficients (R^2), the pseudo first-order model described the kinetic data better than did the pseudo second-order model.

3.3. Equilibrium isotherms

The equilibrium isotherms of phosphate in the slag microspheres are presented in Fig. 4. The equilibrium data were analyzed using the Freundlich, Langmuir, and Langmuir–Freundlich isotherm models represented by the following equations, respectively:

$$q_e = a_F C_e^n \quad (5)$$

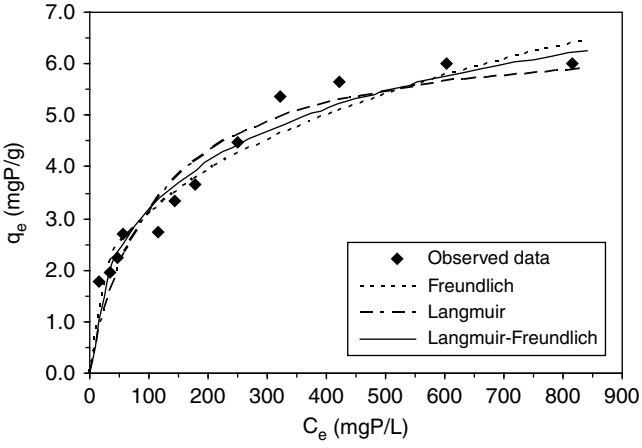

Fig. 4. Equilibrium batch data and model fit for phosphate removal by the slag microspheres.

$$q_e = \frac{q_m a_L C_e}{1 + a_L C_e} \quad (6)$$

$$q_e = \frac{q_m (a_S C_e)^{n_S}}{1 + (a_S C_e)^{n_S}} \quad (7)$$

Here, C_e is the concentration of phosphate in the aqueous solution at equilibrium, a_F is the distribution coefficient, n and n_s are the Freundlich and Langmuir–Freundlich constants, respectively, a_L and a_S are the Langmuir and Langmuir–Freundlich constants related to the binding energy, respectively, and q_m is the maximum mass of phosphate removed per unit mass of the slag microspheres (removal capacity). The parameter values determined by fitting the models to the observed data are provided in Table 3. In the Freundlich model, the distribution coefficient (a_F) was 0.65 l g^{-1} while the Freundlich constant (n) was 0.38. In the Langmuir model, the Langmuir constant (a_L) was 0.009 l mgP^{-1} with a phosphate adsorption capacity (q_m) of 6.65 mgP g^{-1}. In the Langmuir–Freundlich model, the Langmuir–Freundlich constants (a_S and n_S) were 0.002 l mgP^{-1} and 0.56, respectively. The phosphate adsorption capacity (q_m) was determined to be 10.95 mgP g^{-1}. The correlation coefficient (R^2) of the Langmuir–Freundlich model (0.95) was greater than those of the Freundlich (0.94) and Langmuir (0.93) models, indicating that the Langmuir–Freundlich model appropriately describes the equilibrium sorption data. The phosphate adsorption capacity (q_m = 10.95 mgP g^{-1}) is within the values of the other slag adsorbents reported in the literature (0.38–15.70 mgP g^{-1}). For example, Xiong et al. [32] reported that a maximum phosphate adsorption capacity of steel slag

Table 3
Equilibrium isotherm parameters obtained from equilibrium batch experiments for the Freundlich, Langmuir, and Langmuir–Freundlich isotherm models

Freundlich			Langmuir			Langmuir–Freundlich			
a_F (l g^{-1})	n	R^2	q_m (mgP g^{-1})	a_L (l mgP^{-1})	R^2	q_m (mgP g^{-1})	a_s (l mgP^{-1})	n_s	R^2
0.65	0.38	0.94	6.65	0.009	0.93	10.95	0.002	0.56	0.95

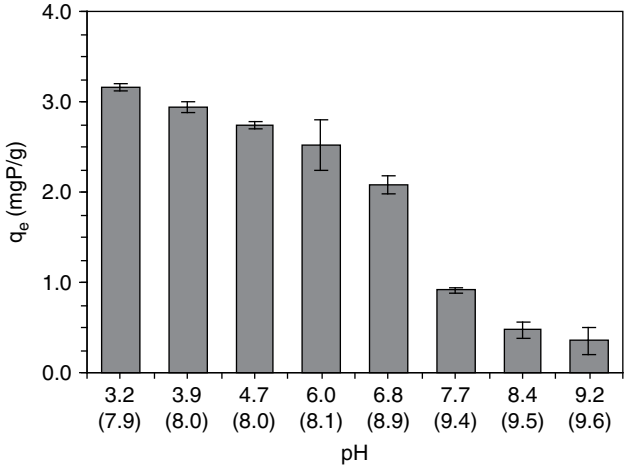

Fig. 5. Effect of solution pH on phosphate removal capacity of the slag microspheres (initial phosphate concentration = 200 mgP l^{-1}). The numbers in parenthesis are the final solution pH values.

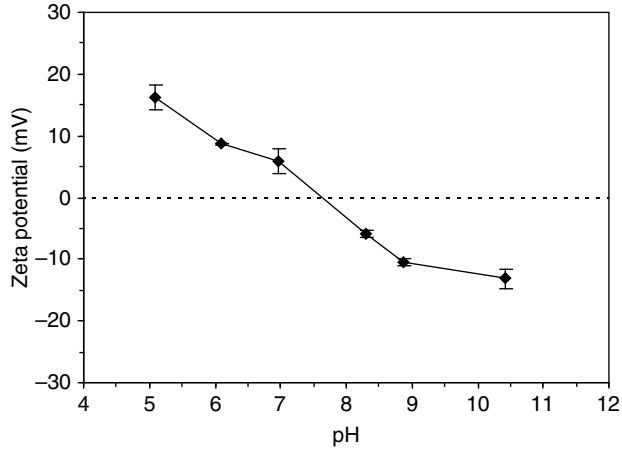

Fig. 6. Zeta potentials of the slag microspheres at different solution pHs.

of 5.3 mgP g^{-1} and Bowden et al. [26] reported a phosphate adsorption capacity of basic oxygen steel slag of 8.39 mgP g^{-1}.

3.4. Effects of solution pH and competing anions

The results of phosphate removal using slag microspheres under various solution pHs are shown in Fig. 5. The phosphate removal was sensitive to pH under the given experimental conditions. The removal capacity (q_e) was the highest at a pH of 3.2 with a value of 3.16 ± 0.04 mgP g^{-1}, which gradually decreased to 2.09 ± 0.10 mgP g^{-1} at a pH of 6.8. Then, the removal capacity dropped sharply to 0.91 ± 0.04 mgP g^{-1} at a pH of 7.7 and decreased continuously to 0.35 ± 0.15 mgP g^{-1} at a pH of 9.2. Overall, the removal capacity decreased one order of magnitude as pH increased from 3.2 to 9.2. Phosphate adsorption on metal surfaces of (Al, Fe) hydroxides decreases with increasing pH [26]. It was demonstrated that the phosphate removal capacity of basic oxygen steel slag increased with increasing pH when phosphate removal occurred through precipitation rather than adsorption [26]. This demonstrates that adsorption to metal hydroxide surfaces plays a major role in our experiments for phosphate removal in the slag microspheres.

The decreasing tendency of the removal capacity with increasing pH obtained in this study agrees well with other the results of other studies [3,6,15]. This phenomenon can be attributed to the surface charges of the slag microspheres. As shown in Fig. 6, the PZC of the slag microspheres was around 7.6. Below the PZC, the microspheres were positively charged and therefore, the adsorption of phosphate anions to the slag microspheres was favorable via electrostatic attractions. As the pH was increased to the PZC, the slag microspheres became less positively charged, causing the adsorption of phosphate to become less favorable. Above the PZC, the slag microspheres became more negatively charged with increasing pH and therefore, the adsorption of phosphate became more unfavorable due to electrostatic repulsion.

During experiments, the solution pH increased and reached a final (equilibrium) pH of 7.9–9.6 (Fig. 5), mainly due to the release of hydroxyl ions (OH^-) from the slag microspheres that were exchanged for phosphate anions. The adsorption of phosphate ions to the slag microspheres can be described by a ligand exchange mechanism [3]. In the adsorption process, phosphate ions can replace OH^- on the surfaces of the slag microspheres, forming inner-sphere complexes including monodentate, bidentate, and binuclear complexes [33,34]. Also, this mechanism can be referred to as a Lewis acid-base interaction in which phosphate ions (Lewis base) are adsorbed on the surface sites (Lewis acid) of the slag microspheres [34,35]. Additionally, electrostatic (Coulombic) interactions can occur between the positively charged surfaces of the slag microspheres and negatively charged phosphate ions, forming an outer-sphere complex [34,36].

The effects of anions (NO_3^-, Cl^-, SO_4^{2-}, and HCO_3^{2-}) on the removal of phosphate in the slag microspheres are shown in Fig. 7. NO_3^-, Cl^-, and SO_4^{2-} had minimal influence on the removal of phosphate in the slag microspheres at concentrations ranging from 0 to 100 mM where the phosphate removal capacity (q_e) remained around 2.75–2.84 mgP g^{-1}. This result is similar to that of a previous report [3] which showed that the influences of NO_3^-, Cl^-, and SO_4^{2-} on the phosphate removal

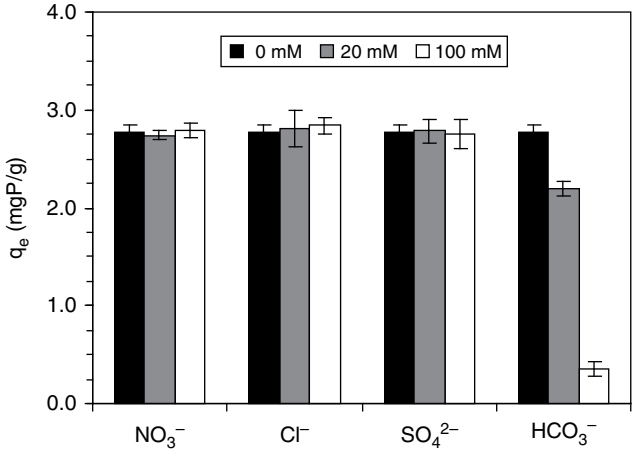

Fig. 7. Effects of competing anions on the phosphate removal capacity of the slag microspheres (initial phosphate concentration = 200 mgP l^{-1}).

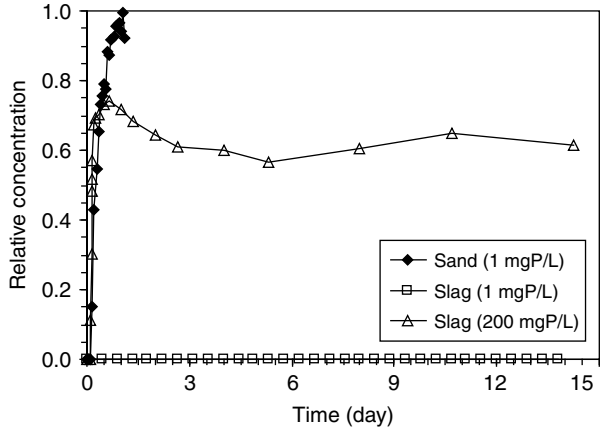

Fig. 8. Breakthrough curves for phosphate removal in the slag microspheres from the column experiments.

in basic oxygen furnace slag were not significant at anion concentrations ranging from 100 to 1000 mg l^{-1}. Meanwhile, bicarbonate (HCO_3^{2-}) greatly interfered with the removal of phosphate in the slag microspheres. At a HCO_3^{2-} concentration of 20 mM, the value of q_e decreased to 2.20 mgP g^{-1}, which is a 21% reduction of the phosphate removal capacity compared to the reduction at 0 mM (2.78 mgP g^{-1}). At a HCO_3^{2-} concentration of 100 mM, the value of q_e decreased further to 0.36 mgP g^{-1} (87% reduction). Our results demonstrate that the slag microspheres could selectively remove phosphate from an aqueous solution. However, the negative impact of HCO_3^{2-} on the phosphate removal in the slag microspheres should be considered.

3.5. Phosphate removal in flow-through columns

The breakthrough curves (BTCs) for phosphate removal by the sand and slag microspheres are presented in Fig. 8. The performance of the slag microspheres in the phosphate removal was compared with that of the sand, the most commonly used as granular filter media. The breakthrough data are presented in terms of the relative concentration of phosphate as a function of time. It should be noted that the slag microspheres (grain size = 0.60–1.18 mm) produced no hydraulic problems (e.g., clogging) in the given experimental conditions. Under conditions of C_0 = 1 mgP l^{-1} and Q = 2.0 ml min^{-1} in sand, the BTC increased sharply, reaching the initial phosphate concentration after around 1 d. Under the same experimental conditions, the BTC for the slag microspheres remained constant at relative concentrations near zero for up to 14 d. At C_0 = 200 mgP l^{-1} and Q = 2.0 ml min^{-1}, the BTC for the slag microspheres increased rapidly, reaching 0.73 of the relative concentration after around 0.5 d and then remained at 0.6–0.7 of the relative concentration for up to 14 d. The removal capacity (q_a) of the slag microspheres in the column experiments was determined to be 2.27 mgP g^{-1} with C_0 = 200 mgP l^{-1}, which is lower than the removal capacities obtained from the batch experiments. Other researchers who conducted column experiments reported a phosphate retention capacity of 1.35 mgP g^{-1} for EAFSS [20] and 8.39 mgP g^{-1} for basic oxygen steel slag [26].

4. Conclusions

In this study, slag microspheres were used to remove phosphate from aqueous solutions. The results of batch experiments indicated that the slag microspheres were effective in the removal of phosphate. The phosphate removal capacity decreased with increasing pH, indicating that adsorption to metal hydroxide surfaces may play a major role in the phosphate removal by the slag microspheres. The decreasing tendency of the removal capacity with increasing pH can be attributed to the surface charge of the slag microspheres, which had a PZC of 7.6. The phosphate removal capacity was not affected by NO_3^-, Cl^-, or SO_4^{2-} but was influenced by bicarbonate. The results of column experiments demonstrated the potential use of the slag microspheres as a granular filter media in flow-through systems for phosphate removal.

Acknowledgments

This research was supported by the National Research Foundation of Korea, funded by the Ministry of Education, Science and Technology, Republic of Korea (grant number 2011–0009688).

References

[1] D.M. Proctor, K.A. Fehling, E.C. Shay, J.L. Wittenborn, J.J. Green, C. Avent, R.D. Bigham, M. Connolly, B. Lee, T.O. Shepker and M.A. Zak, Physical and chemical characteristics of blast furnace, basic oxygen furnace, and electric arc furnace steel industry slags, Environ. Sci. Technol., 34 (2000) 1576–1582.

[2] W. Cha, J. Kim and H. Choi, Evaluation of steel slag for organic and inorganic removals in soil aquifer treatment, Water Res., 40 (2006) 1034–1042.

[3] Y. Xue, H. Hou and S. Zhu, Characteristics and mechanisms of phosphate adsorption onto basic oxygen furnace slag, J. Hazard. Mater., 162 (2009) 973–980.

[4] S.H. Lee, S. Vigneswaran and H. Moon, Adsorption of phosphorus in saturated slag media columns, Sep. Purif. Technol., 12 (1997) 109–118.

[5] K. Sakadevan and H.J. Bavor, Phosphate adsorption characteristics of soils, slags and zeolite to be used as substrates in constructed wetland systems, Water Res., 32 (1998) 393–399.

[6] N.M. Agyei, C.A. Strydom and J.H. Potgieter, The removal of phosphate ions from aqueous solution by fly ash, slag, ordinary Portland cement and related blends, Cement Concrete Res., 32 (2002) 1889–1897.

[7] S. Yim and E.H. Kim, A comparative study of seed crystals for the phosphorus crystallization process, Environ. Technol., 25 (2004) 741–750.

[8] C. Pratt, S. Shilton, S. Pratt, R.G. Haverkamp and N.S. Bolan, Phosphorus removal mechanisms in active slag filters treating waste stabilization pond effluent, Environ. Sci. Technol., 41 (2007) 3296–3301.

[9] V.K. Jha, Y. Kameshima, A. Nakajima and K. Okada, Utilization of steel-making slag for the uptake of ammonium and phosphate ions from aqueous solution, J. Hazard. Mater., 156 (2008) 156–162.

[10] J.P. Gustafsson, A. Renman, G. Renman and K. Poll, Phosphate removal by mineral-based sorbents used in filters for small-scale wastewater treatment, Water Res., 42 (2008) 189–197.

[11] J. Yang, S. Wang, Z. Lu, J. Yang and S. Lou, Converter slag-coal cinder columns for the removal of phosphorous and other pollutants, J. Hazard. Mater., 168 (2009) 331–337.

[12] D. Eveborn, J.P. Gustafsson, D. Hesterberg and S. Hillier, XANES speciation of P in environmental samples: an assessment of filter media for on-site wastewater treatment, Environ. Sci. Technol., 43 (2009) 6515–6521.

[13] H. Sunahara, W.M. Xie and M. Kayama, Phosphate removal by column packed blast furnace slag—I. fundamental research by synthetic wastewater, Environ. Technol., 8 (1987) 589–598.

[14] W.M. Xie, X.C. Zhang, T. Kitaide and H. Sunahara, Phosphate removal by column packed blast furnace slag––II. practical application of secondary effluent, Environ. Technol., 8 (1987) 599–608.

[15] L. Johansson and J.P. Gustafsson, Phosphate removal using blast furnace slags and opoka—mechanisms, Water Res., 34 (2000) 259–265.

[16] E. Oguz, Removal of phosphate from aqueous solution with blast furnace slag, J. Hazard. Mater., B114 (2004) 131–137.

[17] E. Oguz, Thermodynamic and kinetic investigations of PO_4^{3-} adsorption on blast furnace slag, J. Colloid Interface Sci., 281 (2005) 62–67.

[18] A. Hedström and L. Rastas, Methodological aspects of using blast furnace slag for wastewater phosphorus removal, J. Environ. Eng., 132 (2006) 1431–1438.

[19] G. Gong, S. Ye, Y. Tian, Q. Wang, J. Ni and Y. Chen, Preparation of a new sorbent with hydrated lime and blast furnace slag for phosphorus removal from aqueous solution, J. Hazard. Mater., B114 (2009) 714–719.

[20] A. Drizo, Y. Comeau, C. Forget and R.P. Chapuis, Phosphorus saturation potential: a parameter for estimating the longevity of constructed wetland systems, Environ. Sci. Technol., 36 (2002) 4642–4648.

[21] A. Drizo, C. Forget, R.P. Chapuis and Y. Comeau, Phosphorus removal by electric arc steel slag and serpentinite, Water Res., 40 (2006) 1547–1554.

[22] E.H. Kim, S.B. Yim, H.C. Jung and E.J. Lee, Hydroxyapatite crystallization from a highly concentrated phosphate solution using powdered converter slag as a seed material, J. Hazard. Mater., B136 (2006) 690–697.

[23] E.H. Kim, H.K. Hwang and S.B. Yim, Phosphorus removal characteristics in hydroxyapatite crystallization using converter slag, J. Environ. Sci. Health A, 41 (2006) 2531–2545.

[24] E.H. Kim, D.W. Lee, H.K. Hwang and S.B. Yim, Recovery of phosphate from wastewater using converter slag: kinetics analysis of a completely mixed phosphorus crystallization process, Chemosphere, 63 (2006) 192–201.

[25] A.N. Shilton, I. Elmetri, A. Drizo, S. Pratt, R.G. Haverkamp and S.C. Bilby, Phosphorus removal by an 'active' slag filter—a decade of full scale experience, Water Res., 40 (2006) 113–118.

[26] L.I. Bowden, A.P. Jarvis, P.L. Younger and K.L. Johnson, Phosphorus removal from waste waters using basic oxygen steel slag, Environ. Sci. Technol., 43 (2009) 2476–2481.

[27] S.A. Mikhail and A.M. Turcotte, Thermal behaviour of basic oxygen furnace waste slag, Thermochim. Acta, 263 (1995) 87–94.

[28] C.H. Yoon and K.W. Kim, Anatomical descriptions of silicified woods from Madagascar and Indonesia by scanning electron microscopy, Micron, 39 (2008) 825–831.

[29] APHA (American Public Health Association), Standard Methods for the Examination of Water and Wastewater, Washington, DC, 1995.

[30] Y.S. Ho and G. Mckay, Pseudo-second order model for sorption processes, Process Biochem., 34 (1999) 451–465.

[31] T. Mathialagan and T. Viraraghavan, Adsorption of cadmium from aqueous solutions by vermiculite, Sep. Sci. Technol., 38 (2003) 57–76.

[32] J. Xiong, Z. He, Q. Mahmood, D. Liu, X. Yang and E. Islam, Phosphate removal from solution using steel slag through magnetic separation, J. Hazard. Mater., 152 (2008) 211–215.

[33] X.H. Guan, Q. Liu, G.H. Chen and C. Shang, Surface complexation of condensed phosphate to aluminum hydroxide: an ATR-FTIR spectroscopic investigation, J. Colloid Interface Sci., 289 (2005) 319–327.

[34] L.M. Blaney, S. Cinar and A.K. Sengupta, Hybrid anion exchanger for trace phosphate removal from water and wastewater, Water Res., 41 (2007) 1603–1613.

[35] N. Boujelben, J. Bouzid, Z. Elouear, M. Feki, F. Jamoussi and A. Montiel, Phosphorus removal from aqueous solution using iron coated natural and engineered sorbents, J. Hazard. Mater., 151 (2008) 103–110.

[36] M. Arias, J. Da Silva-Carballal, L. Carcía-Río, J. Mejuto and A. Núñez, Retention of phosphorus by iron and aluminum-oxides-coated quartz particles, J. Colloid Interface Sci., 295 (2006) 65–70.